AUTHOR QUERY FORM

Journal: EPSL	**Please e-mail or fax your responses and any corrections to:**
	E-mail: corrections.esch@elsevier.vtex.lt
Article Number: 12079	**Fax: +1 61 9699 6735**

Dear Author,

Please check your proof carefully and mark all corrections at the appropriate place in the proof (e.g., by using on-screen annotation in the PDF file) or compile them in a separate list. Note: if you opt to annotate the file with software other than Adobe Reader then please also highlight the appropriate place in the PDF file. To ensure fast publication of your paper please return your corrections within 48 hours.

For correction or revision of any artwork, please consult *http://www.elsevier.com/artworkinstructions*

Any queries or remarks that have arisen during the processing of your manuscript are listed below and highlighted by flags in the proof. Click on the 'Q' link to go to the location in the proof.

Location in article	Query / Remark: **click on the Q link to go** **Please insert your reply or correction at the corresponding line in the proof**
Q1	Please confirm that given names and surnames have been identified correctly and are presented in the desired order. (p. 1/ line 15)
Q2	Figures 3 and 5 will appear in black and white in print and in color on the web. Based on this, the respective figure captions have been updated. Please check, and correct if necessary. (p. 4/ line 48)
Q3	Please check and correct the citation '(Mogi, ?)'. (p. 4/ line 119)

Please check this box if you have no corrections to make to the PDF file

Thank you for your assistance.   Page 1 of 1

Continuous gravity measurements reveal a low-density lava lake at Kīlauea Volcano, Hawai'i

Daniele Carbone [a,*], Michael P. Poland [b], Matthew R. Patrick [b], Tim R. Orr [b]

[a] Istituto Nazionale di Geofisica e Vulcanologia, Sezione di Catania, Osservatorio Etneo, Catania 95125, Italy
[b] U.S. Geological Survey, Hawaiian Volcano Observatory, PO Box 51, Hawaii National Park, Hawaii 96718-0051, USA

ARTICLE INFO

ABSTRACT

On 5 March 2011, the lava lake within the summit eruptive vent at Kīlauea Volcano, Hawai'i, began to drain as magma withdrew to feed a dike intrusion and fissure eruption on the volcano's east rift zone. The draining was monitored by a variety of continuous geological and geophysical measurements, including deformation, thermal and visual imagery, and gravity. Over the first ∼14 hours of the draining, the ground near the eruptive vent subsided by about 0.15 m, gravity dropped by more than 100 μGal, and the lava lake retreated by over 120 m. We used GPS data to correct the gravity signal for the effects of subsurface mass loss and vertical deformation in order to isolate the change in gravity due to draining of the lava lake alone. Using a model of the eruptive vent geometry based on visual observations and the lava level over time determined from thermal camera data, we calculated the best-fit lava density to the observed gravity decrease — to our knowledge, the first geophysical determination of the density of a lava lake anywhere in the world. Our result, $950 \pm 300 \ \mathrm{kg\,m^{-3}}$, suggests a lava density less than that of water and indicates that Kīlauea's lava lake is gas-rich, which can explain why rockfalls that impact the lake trigger small explosions. Knowledge of such a fundamental material property as density is also critical to investigations of lava-lake convection and degassing and can inform calculations of pressure change in the subsurface magma plumbing system.

© 2013 Elsevier B.V. All rights reserved.

1. Introduction

Lava lakes are a common manifestation of basaltic volcanism around the world and can be persistently active for decades. As a result, they offer opportunities to investigate magma convection, degassing, and other processes that are normally obscured from direct observation (e.g., Tazieff, 1994; Witham and Llewellin, 2006; Spampinato et al., 2008; Oppenheimer et al. 2004, 2009, 2011; Patrick et al., 2011; Orr et al., 2013). In addition, lava lakes represent a significant hazard because of persistent emissions of toxic gases, as exemplified at Kīlauea Volcano, Hawai'i (Elias and Sutton, 2012), as well as the potential for catastrophic draining to feed flank eruptions, which occurred during the 1977 and 2002 eruptions of Nyiragongo Volcano, Democratic Republic of the Congo, and killed hundreds of people (Tedesco et al., 2007; Sawyer et al., 2008).

Active lava lakes around the world have been investigated using a variety of techniques, including gas geochemistry (Sawyer et al., 2008; Oppenheimer et al., 2009), thermal data (Spampinato et al., 2008), textural analysis of erupted products (Carey et al. 2012, 2013), geophysical and visual observations (Palma et al.,

2008; Patrick et al., 2011; Orr et al., 2013), analogue experiments (Witham et al., 2006), and numerical models (Davaille and Jaupart, 1993). Here we introduce a new method to study lava-lake dynamics — continuous gravity. Continuously recording gravity stations have previously been utilized to gain new insights into the accumulation and transport of magma and gas in the shallow parts of active volcanoes (Jousset et al., 2000; Carbone et al. 2006, 2008, 2009, 2012), to image shallow magma convection over time-scales of minutes (Carbone and Poland, 2012), and to detect rapid mass transfer between different elements of a magma plumbing system (Branca et al., 2003). Continuous gravity has not been extensively utilized to measure lava-lake activity, owing mainly to the poor accessibility of most lava lakes. Nevertheless, gravity offers the advantage of quantifying mass change, which is difficult to assess with other methods. When combined with measurements of lava volume change (from visual or deformation measurements), it is possible to estimate lava density. The latter is a critical parameter governing lava-lake convection and degassing (Witham et al., 2006; Carey et al., 2013).

Kīlauea Volcano (Fig. 1) is among the best monitored volcanoes on Earth and has hosted a continuously visible lava lake within an eruptive vent at the volcano's summit since 2010. The excellent accessibility of the lava lake has allowed for collection of diverse datasets, including continuous gravity (Carbone and Poland, 2012),

* Corresponding author.
E-mail address: carbone@ct.ingv.it (D. Carbone).
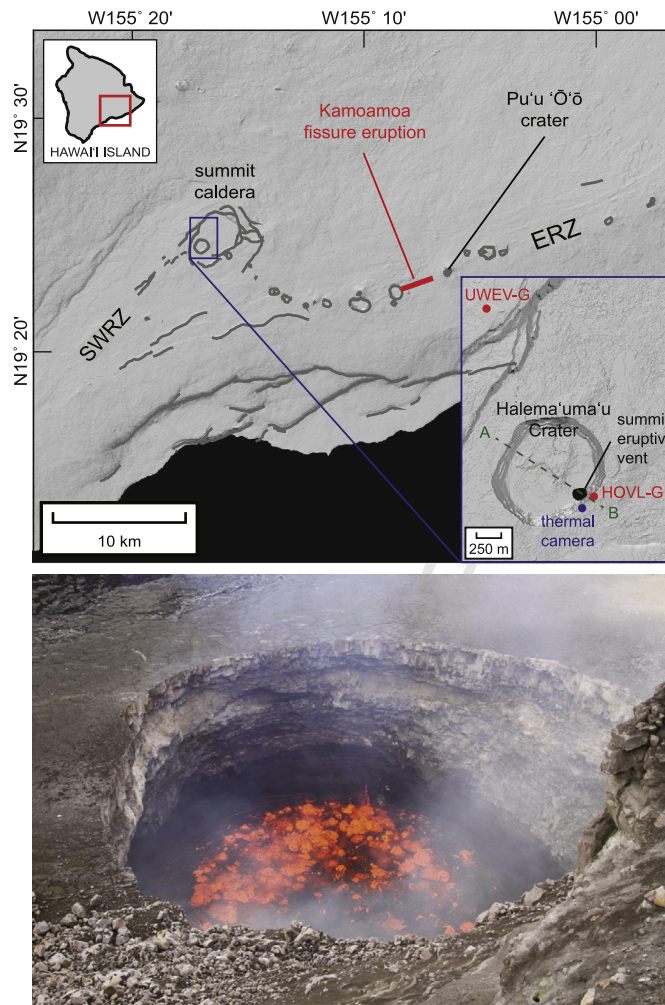
Fig. 1. (Top) Map of Kīlauea showing the locations of Pu'u 'Ō'ō eruptive vent, Kamoamoa eruptive fissure, east rift zone (ERZ), southwest rift zone (SWRZ), and summit caldera. Inset gives locations of the summit eruptive vent on the east margin of Halema'uma'u Crater, thermal camera (blue dot), and gravimeters (red dots; GPS station HOVL is co-located with gravimeter HOVL-G). A–B shows cross section used in Fig. 4a. (Bottom) Photo of lava lake in summit eruptive vent taken from about 50 m southwest of the thermal camera. USGS photograph taken by T. Orr on March 3, 2011.

deformation (Lundgren et al., 2013), and visual imagery (Orr et al., 2013). We present the first geophysical determination of the density of a lava lake by combining continuous gravity data with lava-level measurements collected during draining of Kīlauea's summit lava lake in March 2011. Our results indicate that a lava density of slightly more than one-third of typical basaltic magma is required to fit the magnitude of the gravity decrease given the lava level over time and observed vent geometry. The Kīlauea lava lake is therefore gas-rich, which has important implications for convection, magma reservoir pressure, and hazards.

2. Kīlauea's 2008 – present summit eruption

On 19 March 2008, a small explosion occurred from the east margin of Halema'uma'u Crater within Kīlauea Caldera (Fig. 1), marking the first summit eruption at Kīlauea since 1982 and the first explosion at the summit since 1924 (Wilson et al., 2008; Houghton et al., 2011). Additional explosions occurred throughout 2008, depositing ash, lapilli, and occasional bombs on the rim of Halema'uma'u Crater (Wooten et al., 2009). After the opening of the vent, all explosions were associated with collapse of the vent rim and walls as the vent grew from an initial diameter of 35 m (Orr et al., 2013) to dimensions of about 160 m by 220 m by March 2013 (as determined from ground-based lidar surveys). The presence of lava at shallow levels was inferred from the ejection of juvenile ash, lapilli, and spatter (Wooten et al., 2009), but the lava lake was not observed until September 2008. At that time, the vent had grown large enough to enable views down to the lava surface, which, at times, was more than 200 m below the floor of Halema'uma'u Crater (Orr et al., 2013). The lava-lake elevation gradually rose to about 62 m below the vent rim by early 2011. Small-scale fluctuations of up to a few tens of meters over hours to minutes due to variations in degassing behavior (Patrick et al., 2011) were superimposed on the overall trend of increasing elevation. Kīlauea's summit vent has been characterized by persistent degassing and minor ash emission since its formation (Swanson et al., 2009; Houghton et al., 2011). Throughout the entire summit eruption sequence, Kīlauea's east rift zone (ERZ) eruption, which started in 1983 (Fig. 1; Heliker and Mattox, 2003), has continued unabated. Gas emissions from the ERZ have decreased since 2008, however, presumably in part because some magma erupting from the ERZ has previously degassed at the summit (Elias and Sutton, 2012).

A new episode of ERZ eruptive activity began on the local afternoon of 5 March 2011 (GMT time = 23:42) with the onset of a seismic swarm just uprift of Pu'u 'Ō'ō — the main ERZ eruptive vent. At the same time, rapid deflation was detected by tiltmeters at the summit and Pu'u 'Ō'ō, suggesting withdraw of magma from both locations to feed a growing dike. About three hours later the dike reached the surface at a point 2–3 km uprift of Pu'u
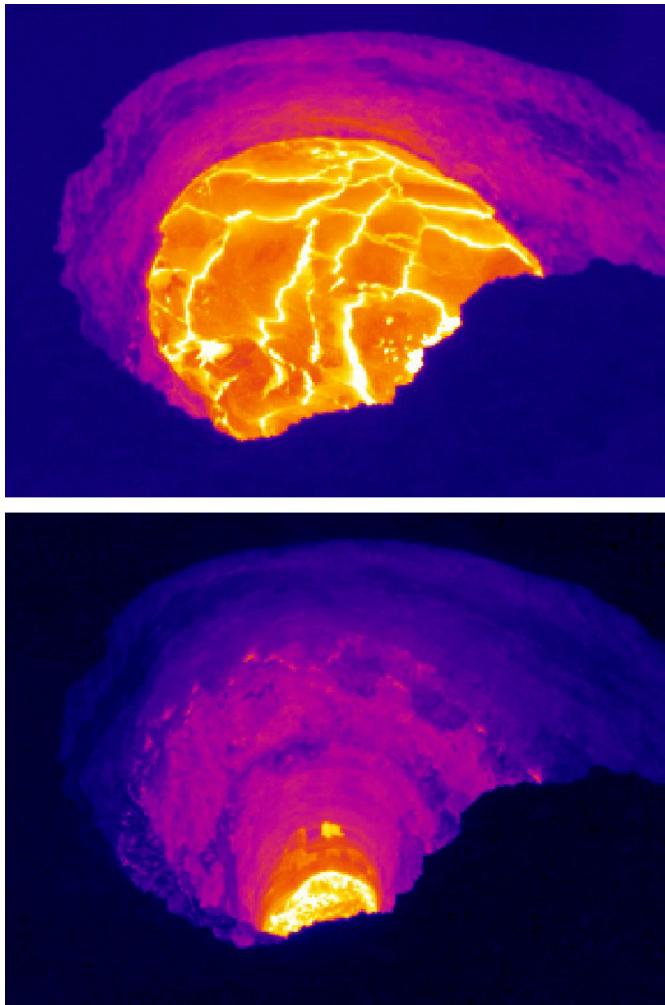
Fig. 2. Thermal camera images of Kīlauea's summit lava lake. The lava level dropped by approximately 140 meters between the times of the top (22:30 GMT on 4 March 2011) and bottom (16:30 GMT on 6 March 2011) images. View is from approximately the same location as the photo in Fig. 1.

ʻŌʻō, starting the 4.5-day-long Kamoamoa fissure eruption (Fig. 1; Lundgren et al., 2013). The intrusion and eruption were accompanied by collapse of Puʻu ʻŌʻō as magma withdrew from beneath the crater to feed the new eruptive fissure. Magma likewise drained from beneath the summit, causing a rapid lowering of the level of the summit lava lake (Fig. 2). Within 24 h of the start of the ERZ seismic swarm, the lava level in the summit had dropped by over 140 m, amounting to a volume of about 2.5×10^6 m^3 of lava. Summit deflation measured by GPS tracked the lava-level drop (Fig. 3a) and was modeled as due to volume loss in a reservoir located about 1.7 km beneath the east margin of Halemaʻumaʻu Crater (Lundgren et al., 2013). Deflation at both the summit and Puʻu ʻŌʻō gradually waned as the eruption progressed. The eruption ended at about 08:00 GMT on March 10, and inflationary tilt began at the summit and Puʻu ʻŌʻō. Over the ensuing weeks, the lava level within the summit gradually rose, tracking summit inflation. The ERZ eruption resumed at Puʻu ʻŌʻō on March 26.

3. Data

Kīlauea's summit lava lake is monitored by a variety of instrumentation, including camera, GPS, and continuous gravity stations on the rim of Halemaʻumaʻu Crater, immediately adjacent to the summit vent. Combining these data over the course of lake withdrawal allowed us to calculate the bulk density of the lava lake.

3.1. GPS data

Deformation associated with the Kamoamoa eruption was recorded by a network of GPS stations across Kīlauea, as described by Lundgren et al. (2013). The closest GPS station to the summit eruptive vent is HOVL, located about 20 m east of the east rim of Halemaʻumaʻu Crater (Fig. 1). Data from HOVL are collected at 1 Hz and were processed using the RTNet (Real Time Network) software to achieve 1 s solutions. A low-pass filter with a cut-off frequency of 1.2×10^{-5} Hz was used to reduce noise associated with the raw 1 s data. Vertical deformation at HOVL indicates subsidence that reached 0.15 m within 12 hours of the start of the Kamoamoa fissure eruption (Fig. 3a).

3.2. Thermal imagery

The drop in lava level over time (Figs. 2 and 3b) was tracked by a thermal camera on the rim of Halemaʻumaʻu Crater (Figs. 1, 2, and Supplementary movie) that provided a continuous view of the lava lake. Thermal imagery was acquired by a Mikron M7500 infrared camera overlooking the summit eruptive vent (Patrick et al., 2012). The camera has a horizontal field of view of 53° and an image size of 320×240 pixels. Images were acquired every 5 s and transmitted to the observatory in real time. The lava level was calculated every hour from thermal camera measurements. The level of the lake (in image pixels) was measured by eye where the lake intersected the back wall of the crater. Each level measurement in image coordinates was converted to depth in meters using two end-member tie points. The first was a direct measurement of the lava level using a laser range-finder on 2 March 2011, prior to the lava-lake draining. The second measurement was taken on 7 March (when lava was at its deepest point), using a theodolite and exploiting proxy measurements of features in line with the deepest point inside the vent (from the point of view of the thermal camera and a visible light camera operating 60 m to the north). Triangulation from these two locations allowed us to determine horizontal distances to the back wall of the vent, and vertical angles allowed us to calculate the depth of the lava. We assume an overall error in our depth measurements of 5% of the depth beneath the floor of Halemaʻumaʻu Crater based on (a) the standard deviation of multiple theodolite measurements that were used to calculate the distance between the thermal camera and the back wall of the vent (about 3 m) and (b) the uncertainty associated with picking the pixel interface between the lava and back wall of the vent in thermal camera images.

3.3. Gravity data

Two continuously operating gravimeters were located at the summit of Kīlauea at the time of the Kamoamoa eruption: one near the Hawaiian Volcano Observatory on the western rim of the caldera, about 2 km from the summit eruptive vent (UWEV-G in Fig. 1), and another on the rim of Halemaʻumaʻu Crater, about 80 m above the crater floor and 150 m east of the center of the summit eruptive vent (HOVL-G in Fig. 1; Carbone and Poland, 2012). HOVL-G is equipped with a LaCoste and Romberg gravimeter (G-721) upgraded with the Aliod-100 electronic feedback system. Gravity, time, instrument temperature, voltage, long level, and cross level are recorded at 0.5 s intervals and resampled to 1 s. UWEV-G is equipped with a ZLS Burris instrument (B-41), which samples every 10 s. Data from both instruments were corrected for the effect of gravity Earth tides through the Eterna33 software package. HOVL-G recorded a gravity decrease during the lava-level drop that tracked both lava level and surface deformation, reaching a magnitude of more than 100 μGal within 20 hours of the onset of lake draining (Fig. 3c). Conversely, data from UWEV-G
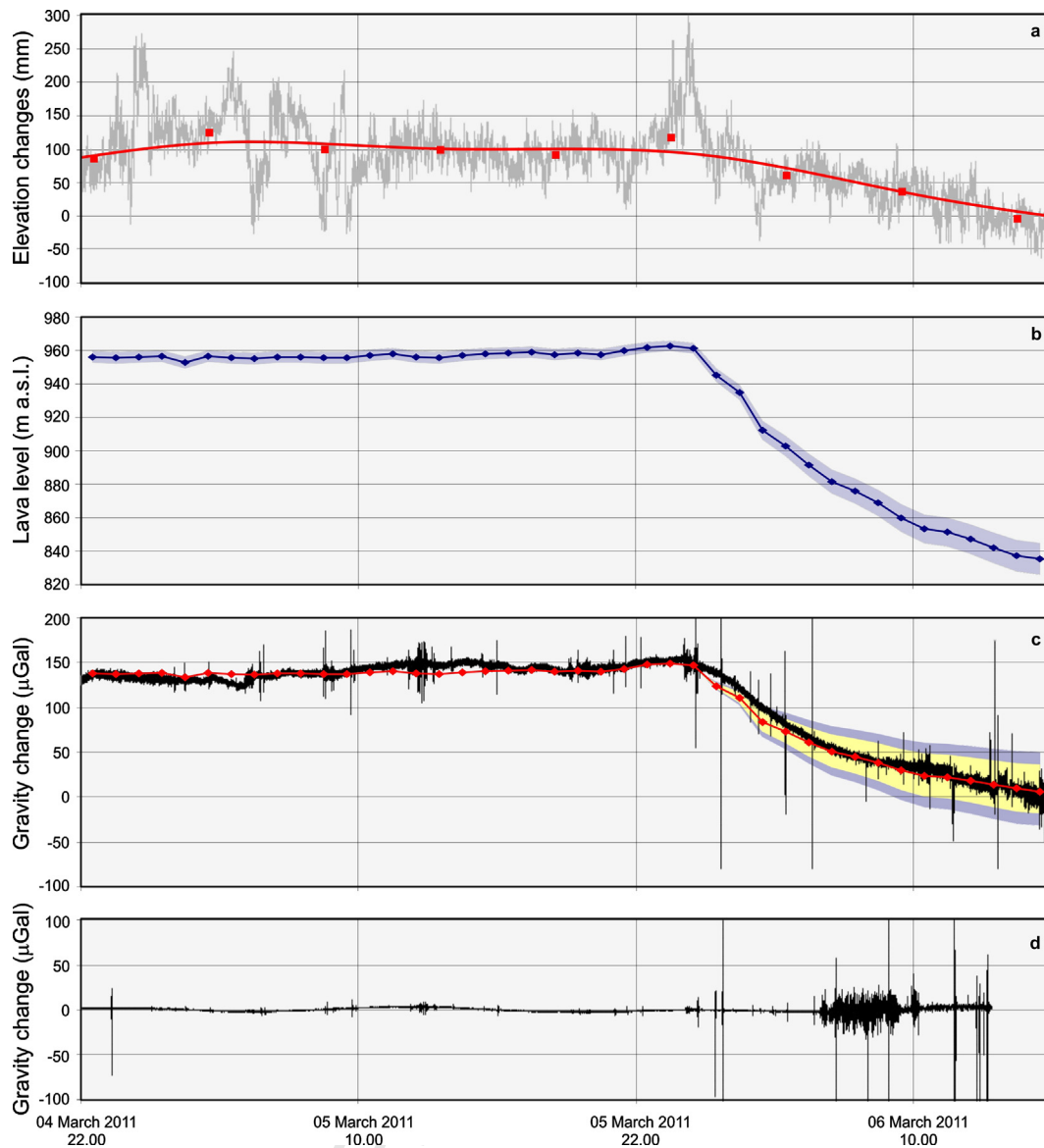
Fig. 3. (a) Vertical deformation from GPS station that is co-located with the HOVL-G gravimeter. Gray line is raw 1 s data and red line is low-pass-filtered (cutoff = 1.2×10^{-5} Hz) signal that is used to correct the gravity data for elevation and subsurface mass change. Red dots are 5-h average positions. (b) Lava level as determined from thermal camera data. The shaded blue area gives the uncertainty on the level during lava draining (approximately 5% of the depth beneath the floor of Halemaʻumaʻu Crater). (c) Adjusted (Eq. (1)) gravity data (black curve) from HOVL-G station and calculated gravity change (red curve, with diamonds for hourly values) based on lava level in panel (b) and assuming a density of 950 kg m^{-3}. The shaded areas represent gravity changes calculated assuming densities 200 and 300 kg m^{-3} (yellow and blue areas, respectively) lower and higher (upper and bottom ends of the ranges, respectively) than the 950 kg m^{-3} value. (d) Gravity data from UWEV-G station. (For interpretation of the references to color in this figure legend, the reader is referred to the web version of this article.)

show no change during the lava-lake draining and summit defla-
tion, although high noise levels due to increased seismicity and
ground motion occurred a few hours after the onset of draining,
and the data stream eventually failed (about 12 h after draining
began; Fig. 3d). The strong drop measured at HOVL-G and absence
of a similar signal at UWEV-G indicate that the gravity decrease
was a local phenomenon, restricted to the immediate vicinity of
the summit eruptive vent. We therefore do not consider data from
UWEV-G in our analysis of mass loss due to lava-lake withdrawal.

The HOVL-G gravity signal reflects a combination of three
processes. First, subsidence due to summit deflation moved the
gravimeter closer to the center of the Earth, resulting in a grav-
ity increase. Second, mass removal from the 1.7-km-deep magma
reservoir, which deflated during the dike intrusion and eruption
(Lundgren et al., 2013), caused a gravity decrease. Third, drop in
the level of the lava lake was associated with a mass loss in the
vicinity of the gravimeter, and thus a gravity decrease.

4. Gravity data adjustments

Based on the vertical GPS data and assuming a simple point
source of pressure change (Mogi, **?**), which was used to model
summit deflation during the Kamoamoa eruption (Lundgren et al.,
2013), the first two processes affecting the HOVL-G gravity signal
— namely subsidence and mass removal from the magma reservoir
— can be evaluated through the relation (Eggers, 1987):

$$\Delta g = \frac{4}{3}\pi G \rho \Delta h - \beta \Delta h \tag{1}$$

where Δh is the elevation change, G is the gravitational con-
stant (6.67×10^{-11} m^3 kg^{-1} s^{-2}), ρ is magma density (2300–2700
kg m^{-3}), and $\beta \Delta h$ is the free-air gradient (-308.6 μGal m^{-1}).
The first term ($\frac{4}{3}\pi G \rho \Delta h$) gives the gravity change due to subsur-
face mass loss from a point source, while the second term ($\beta \Delta h$)
describes gravity change due to vertical deformation (the free-
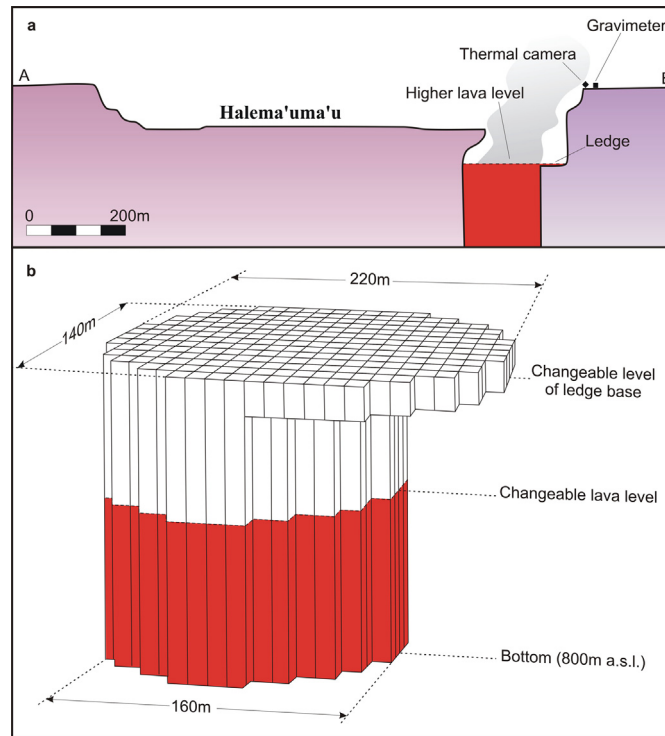
Fig. 4. (a) Schematic cross section (redrawn from Orr et al., 2013) through Halema'uma'u Crater and the summit eruptive vent (trace A–B in Fig. 1) showing vent shape as deduced from visual observations. (b) Model geometry consisting of 252 vertical square-based (10 × 10 m) parallelepipeds with changeable height to simulate varying lava levels. The shape of the model is intended to reproduce the asymmetric shape of the eruptive vent.

air effect). In the case under study here, a maximum elevation change (Δh) of −0.15 m (subsidence) was observed (Section 3.1 and Fig. 3a). Using this value, Eq. (1) predicts gravity effects for mass loss and subsidence of about −11 μGal and 46 μGal, respectively, resulting in a net effect of about 35 μGal. The positive sign of this effect implies a negative adjustment and, thus, a greater amplitude of the gravity decrease due to draining of the lava lake. Using the filtered GPS data (Fig. 3a), we calculated the gravity effect of mass loss and subsidence over time and subtracted this value from the HOVL-G gravity time series, which increased the magnitude of the overall change and revealed the magnitude of the signal due to the lava-level drop within the summit vent (Fig. 3c). This adjustment depends on several assumptions, including the magnitude of the free-air gradient (measured at Kīlauea by Johnson, 1992, and Kauahikaua and Miklius, 2003), the treatment of magma as an incompressible fluid (Johnson et al., 2000; Rivalta and Segall, 2008), and spherical magma storage geometry (Gudmundsson, 1986). Varying these parameters, however, results in only minor changes in the calculated adjustment — a small percentage of the overall gravity variation. We are therefore confident that our adjusted time series is a good representation of the gravity change due solely to draining of the lava lake.

5. Modeling lava-lake density

To investigate the gravity effect produced by the lava-level drop, we developed a numerical model of the vent that takes into account its geometry as deduced from visual observations (Figs. 1, 2, and 4a) and ground-based lidar data. The vent shape is approximated by an elliptical cylinder which widens abruptly at the top. The bottom of the vent cavity measures 140 m (minor axis) by 160 m (major axis). The major axis increases to 220 m in the upper part of the vent, forming a "ledge" that is sometimes briefly flooded by episodic small changes in lava-lake level. The model

consists of 252 vertical square-based (10 × 10 m) parallelepipeds with changeable height (Fig. 4b). The gravity effect produced by each parallelepiped is calculated (Talwani, 1973), and the total effect is obtained by summing their contributions. Since we are only interested in the relative changes during the lava-lake draining, we fixed a bottom (reference) for our model that is below the lowest lava level observed (about 800 m a.s.l., which occurred on 7 March 2011), while the top of the model is the highest level reached by the lava lake during the studied interval (about 960 m a.s.l.; Figs. 3b, 4b). The model geometry accounts for the wider upper portion of the vent as deduced from visual observations; however, since we do not have precise knowledge of the elevation of the ledge at the time of the lava draining (the ledge was built up as the lava lake rose in elevation in early 2011), we allow this parameter to vary in our calculations. By varying the height of the parallelepipeds above the reference level, it is possible to simulate the gravity effect due to the lava-level changes in the vent.

The residual gravity changes shown in Fig. 3c are due to the mass loss in the uppermost part of the summit vent caused by the drop in the level of the lava lake. In particular, the observed gravity changes are a function of (i) the amount of mass lost from the source, (ii) the shape of the source and (iii) the distance between the source and the observation point. In our case, only (i) is unknown and, since we can determine the volume of the source from the available geometrical information, the only parameter to be estimated is the density of the material filling the vent. Using the lava level determined from the thermal camera, we performed a calculation aimed at assessing the value of lava density that yields the best fit to the gravity changes. This calculation was restricted to the interval between 22:00 on 4 March and 16:00 on 6 March (GMT times). Afterwards, ground shaking associated with volcanic activity may have affected the gravity signal by inducing data tares and greater noise. We therefore did not include the signal after 16:00 on 6 March (GMT) in the calculation.
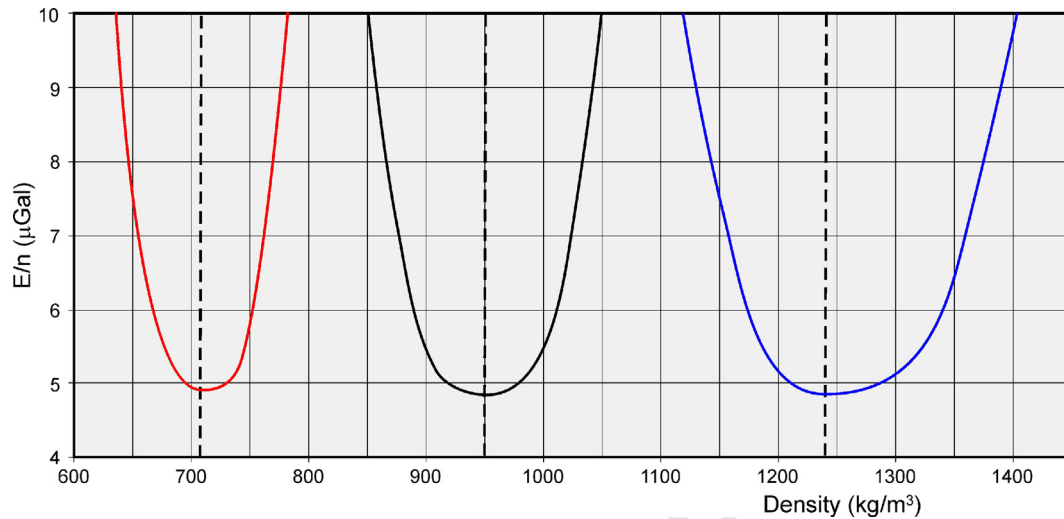
Fig. 5. Curves showing how the average misfit between observed and calculated gravity data changes as a function of the density assumed for the lava in the vent. The three curves are calculated assuming different input parameters to the modeling scheme. Black curve: vent size and distance between source and observation point as deduced from visual observations; lava-level data as calculated from thermal camera images. Blue curve: vent size and distance between source and observation point 10% smaller and longer, respectively, than the values deduced from visual observation; lava-level data on the upper end of the uncertainty range (Fig. 3b). Red curve: vent size and distance between source and observation point 10% bigger and shorter, respectively, than the values deduced from visual observation; lava-level data on the lower end of the uncertainty range (Fig. 3b). Taking into account possible errors on the model parameters, the uncertainty on our density estimate is ±300 kg m^{-3}. For each set of input parameters, the average misfit ($E(\rho)/n$) is always less than 5 μGal. (For interpretation of the references to color in this figure legend, the reader is referred to the web version of this article.)

We identified the best-fit density as the one that provides the lowest misfit between observed and modeled gravity data. The misfit is defined as:

$$E(\rho) = \sum_{i=1}^{n} \left| x_i^{obs} - x_i^{calc} \right| \tag{2}$$

where x_i^{obs} is the observed gravity value at the time t_i, x_i^{calc} is the corresponding calculated value, and n is the number of points in both the observed and calculated time sequences.

The time sequence of lava levels used as input to the modeling scheme was sampled at 1 hour intervals. The model produces a synthetic gravity sequence at the same sampling rate. Resampling of the observed gravity sequence from 1 sample/s to 1 sample/h was thus necessary to calculate $E(\rho)$. Resampling was accomplished by averaging over a 1-h-long sliding time window. For each step, the resulting point was attached to the center time of the window.

Our results indicate that lava with an average density of about 950 kg m^{-3} occupied the upper 120 m of the vent at the time of the draining (Figs. 3c and 5). Our best fit also suggests an inconsequential thickness (on the order of 1 m) for the upper part of the lake. Indeed, the assumption of a larger upper portion (Fig. 4) of any significant height always resulted in a poorer fit between observed and modeled gravity data. This result implies that the ledge was at an elevation almost equal to the highest level reached by the lava during the studied period — a conclusion that is consistent with visual observations during lake draining.

We performed a bound analysis to evaluate the variation in the best-fit density when model parameters are changed. Specifically, we defined bounds on (1) the lava-level changes retrieved from thermal camera images (Fig. 3b), (2) the size of the model source (i.e., the eruptive vent) and (3) the distance between source and observation point. For (1), uncertainty in the measurement results from an imperfect knowledge of the vent geometry. The height of the lava immediately prior to draining was determined by visually estimating that the level had risen by 3 m above that measured by laser ranger-finder on 2 March, and it is accurate to within about 1 m. The minimum lake elevation, however, requires knowledge of the distance between the thermal camera and the far wall of the vent to calculate the lake elevation from the thermal images. Uncertainty in this parameter corresponds to potential error in the measurement of the lowest lava level of ± 10 m. Error in lava level therefore increases with depth (Fig. 3b). As for (2) and (3), relying on the uncertainty for the visual observations on which the geometrical parameters are based, we consider, for both source size and distance to the observation point, values that are 10% larger and smaller than those used in the model. With these bounds on lava level, vent geometry, and vent location, we calculated the best-fit densities that correspond to the edge configurations. For example, if the vent size and distance between source and observation point are 10% smaller and longer, respectively, than the values deduced from visual observations, and if the lava level over time is along the upper end of the uncertainty range (Fig. 3b), a best-fit density of 1240 kg m^{-3} results (blue curve in Fig. 5). Our bound analysis indicates that the best-fit density of the lava in the vent may take minimum and maximum values that differ by up to ±300 kg m^{-3} from the best-fit 950 kg m^{-3} estimate (Fig. 5).

6. Discussion and conclusions

That the modeled density of the lava lake is about the same as that of water may seem a surprising result, but it is consistent with other independent measurements. Ejecta from a small explosive eruption on 9 April 2008, caused by the collapse of a portion of the vent wall, has a bimodal density distribution with a range of 500–2000 kg m^{-3}, but with the greatest number of clasts having a density of 800 kg m^{-3} (Carey et al., 2013). About two-thirds of measured clasts ejected during a different explosion, on 12 October 2008, had densities of 500–800 kg m^{-3} (Carey et al., 2012). Similar results were found at Stromboli, where average ejecta density for several explosions in 2002 was in the range of 900–1200 kg m^{-3} (Lautze and Houghton, 2007).

The density of the lava within the summit vent is the critical variable in calculations of lava-lake convection and magma pressure. That the lava lake is convecting is clear from the persistence of gas emissions without significant lava effusion (Oppenheimer et al. 2009, 2011) and the motion of the lake's surface (Carey et

al., 2013). Microtextural analysis suggests convection to a depth of 300 m assuming a lava-lake density of 1000 kg m^{-3}. A lower density (which is possible considering the lower bound on our model result) would imply that the convection reaches even deeper — possibly to depths where small magma storage areas may exist (Cervelli and Miklius, 2003).

Pressure variations within Kīlauea's shallow magmatic system are indicated by changes in lava-lake level. Magma pressure is typically inferred only from deformation models that assume a magma reservoir geometry (McTigue, 1987) and do not account for magma compressibility due to the presence of volatiles (e.g., Johnson et al., 2000; Rivalta and Segall, 2008). Lava-lake height changes, however, are a direct measure of pressure through $\rho g \Delta h$, and lake density (ρ) is the most critical parameter because g is a constant and Δh can be observed directly. Our lava-lake density calculation is therefore fundamental to any analysis of the dynamics of the lava lake and associated magma system.

Hazards associated with lava lakes can be both localized (from small explosions; Carey et al., 2012; Orr et al., 2013) and far-reaching (due to persistent gas emissions; Poland et al., 2009; Patrick et al., 2011). Near-surface gas accumulation within the lava lake has been hypothesized to explain both the mechanism for lava rise/fall events, as well as catastrophic overturn and small explosions that often accompany rockfalls (Patrick et al., 2011; Orr et al., 2013). The low density we measure indicates that, at the time of the March 2011 lava-level drop, more than half of the lava-filled vent volume was occupied by exsolved gas. This figure supports the gas accumulation model for episodic changes in lava level (Patrick et al., 2011) and emphasizes the large quantity of gas that is primed for release if the lake surface is disturbed by a rockfall or other event (Orr et al., 2013).

Our results demonstrate the value of applying continuous gravity measurements at other lava lakes to determine density, lava level, and other parameters. Indeed, density is a critical parameter in models of lava-lake behavior, and incorrect estimates can lead to biased calculations of the scales of convection time (Oppenheimer et al., 2009) and cell-size (Carey et al., 2013). Models of continuous gravity may also indicate changes in lava-lake density over time, which will be useful in forecasting the future evolution of volcanic activity and hazards. Finally, we have demonstrated the utility of continuous gravity data as a tool for monitoring mass transfer from a lava lake to other parts of the magma plumbing system — information that is especially valuable when continuous, real-time observation of a lava lake is not possible.

Acknowledgements

Appendix A. Supplementary material

Supplementary material related to this article can be found online at http://dx.doi.org/10.1016/j.epsl.2013.06.024.

References

Branca, S., Carbone, D., Greco, F., 2003. Intrusive mechanism of the 2002 NE-Rift eruption at Mt. Etna (Italy) inferred through continuous microgravity data and volcanological evidences. Geophys. Res. Lett. 30 (20), http://dx.doi.org/10.1029/2003GL018250. 2077.

Carbone, D., Poland, M.P., 2012. Gravity fluctuations induced by magma convection at Kīlauea Volcano, Hawai'i. Geology 40 (9), 803–806.

Carbone, D., Zuccarello, L., Saccorotti, G., Greco, F., 2006. Analysis of simultaneous gravity and tremor anomalies observed during the 2002–2003 Etna eruption. Earth Planet. Sci. Lett. 245, 616–629.

Carbone, D., Zuccarello, L., Saccorotti, G., 2008. Geophysical indications of magma uprising at Mt Etna during the December 2005 to January 2006 non-eruptive period. Geophys. Res. Lett. 35, L06305, http://dx.doi.org/10.1029/2008GL033212.

Carbone, D., Jousset, P., Musumeci, C., 2009. Gravity "steps" at Mt. Etna volcano (Italy): Instrumental effects or evidences of earthquake-triggered magma density changes? Geophys. Res. Lett. 36, L02301, http://dx.doi.org/10.1029/2008GL036179.

Carbone, D., Zuccarello, L., Montalto, P., Rymer, H., 2012. New geophysical insight into the dynamics of Stromboli volcano (Italy). Gondwana Res. 22, 290–299, http://dx.doi.org/10.1016/j.gr.2011.09.007.

Carey, R.J., Manga, M., Degruyter, W., Swanson, D., Houghton, B., Orr, T., Patrick, M., 2012. Externally triggered renewed bubble nucleation in basaltic magma: The 12 October 2008 eruption at Halema'uma'u Overlook vent, Kīlauea, Hawai'i, USA. J. Geophys. Res. 117, B11202.

Carey, R.J., Manga, M., Degruyter, W., Gonnermann, H., Swanson, D., Houghton, B., Orr, T., Patrick, M., 2013. Convection in a volcanic conduit recorded by bubbles. Geology 41, 395–398.

Cervelli, P.F., Miklius, A., 2003. The shallow magmatic system of Kīlauea Volcano. In: Heliker, C., Swanson, D.A., Takahashi, T.J. (Eds.), The Pu'u 'Ō'ō-Kūpaianaha Eruption of Kīlauea Volcano, Hawai'i: The First 20 Years. In: U.S. Geol. Surv. Prof. Pap., vol. 1676, pp. 149–163 (Chap. 9).

Davaille, A., Jaupart, C., 1993. Thermal convection in lava lakes. Geophys. Res. Lett. 20 (17), 1827–1830.

Eggers, A.A., 1987. Residual gravity changes and eruption magnitudes. J. Volcanol. Geotherm. Res. 33, 201–216.

Elias, T., Sutton, A.J., 2012. Sulfur dioxide emission rates from Kīlauea Volcano, Hawai'i, 2007–2010. U.S. Geol. Surv. Open-File Rep. 2012–1107.

Gudmundsson, A., 1986. Mechanical aspects of postglacial volcanism and tectonics of the Reykjanes Peninsula, Southwest Iceland. J. Geophys. Res. 91, 12711–12721.

Heliker, C., Mattox, T.N., 2003. The first two decades of the Pu'u 'Ō'ō-Kūpaianaha eruption: Chronology and selected bibliography. In: Heliker, C., Swanson, D.A., Takahashi, T.J. (Eds.), The Pu'u 'Ō'ō-Kūpaianaha Eruption of Kīlauea Volcano, Hawai'i: The First 20 Years. In: U.S. Geol. Surv. Prof. Pap., vol. 1676, pp. 1–27 (Chap. 1).

Houghton, B.F., Swanson, D.A., Carey, R.J., Rausch, J., Sutton, A.J., 2011. Pigeonholing pyroclasts: Insights from the 19 March 2008 explosive eruption of Kīlauea volcano. Geology 39, 263–266.

Johnson, D.J., 1992. Dynamics of magma storage in the summit reservoir of Kīlauea Volcano, Hawaii. J. Geophys. Res. 97, 1807–1820.

Johnson, D.J., Sigmundsson, F., Delaney, P.T., 2000. Comment on "Volume of magma accumulation or withdrawal estimated from surface uplift or subsidence with application to the 1960 collapse of Kīlauea Volcano" by P.T. Delaney and D.F. McTigue. Bull. Volcanol. 61, 491–493.

Jousset, P., Dwipa, S., Beauducel, F., Duquesnoy, T., Diament, M., 2000. Temporal gravity at Merapi during the 1993–1995 crisis: An insight into the dynamical behaviour of volcanoes. J. Volcanol. Geotherm. Res. 100, 289–320.

Kauahikaua, J., Miklius, A., 2003. Long-term trends in microgravity at Kīlauea's summit during the Pu'u 'Ō'ō-Kūpaianaha eruption. In: Heliker, C., Swanson, D.A., Takahashi, T.J. (Eds.), The Pu'u 'Ō'ō-Kūpaianaha Eruption of Kīlauea Volcano, Hawai'i: The First 20 Years. In: U.S. Geol. Surv. Prof. Pap., vol. 1676, pp. 165–171 (Chap. 10).

Lautze, N.C., Houghton, B.F., 2007. Linking explosion intensity and magma rheology at Stromboli volcano in 2002. Bull. Volcanol. 69, 445–460.

Lundgren, P.L., Poland, M., Miklius, A., Orr, T., Yun, S., Fielding, E., Liu, Z., Tanaka, A., Szeliga, W., Hensley, S., Owen, S., 2013. Evolution of dike opening during the March 2011 Kamoamoa fissure eruption, Kīlauea Volcano, Hawai'i. J. Geophys. Res. 118, http://dx.doi.org/10.1002/jgrb.50108.

McTigue, D.F., 1987. Elastic stress and deformation near a finite spherical magma body: Resolution of the point source paradox. J. Geophys. Res. 92, 12931–12940.

Oppenheimer, C., McGonigle, A.J.S., Allard, P., Wooster, M.J., Tsanev, V.I., 2004. Sulfur, heat and magma budget of Erta 'Ale lava lake, Ethiopia. Geology 32, 509–512.

Oppenheimer, C., Lomakina, A.S., Kyle, P.R., Kingsbury, N.G., Boichu, M., 2009. Pulsatory magma supply to a phonolite lava lake. Earth Planet. Sci. Lett. 284 (3–4), 392–398.

Oppenheimer, C., Moretti, R., Kyle, P.R., Eschenbacher, A., Lowenstern, J.B., Hervig, R.L., Dunbar, N.W., 2011. Mantle to surface degassing of alkalic magmas at Erebus volcano, Antarctica. Earth Planet. Sci. Lett. 306 (3–4), 261–271.

Orr, T.R., Thelen, W.A., Patrick, M.R., Swanson, D.A., Wilson, D.C., 2013. Explosive eruptions triggered by rockfalls at Kīlauea volcano, Hawai'i. Geology 41, 207–210.

Palma, J., Calder, E.S., Basualto, D., Blake, S., Rothery, D.A., 2008. Correlations between SO₂ flux, seismicity, and outgassing activity at the open vent of Villarrica volcano, Chile. J. Geophys. Res. 113, B10201.

Patrick, M., Wilson, D., Fee, D., Orr, T., Swanson, D., 2011. Shallow degassing events as a trigger for very-long-period seismicity at Kīlauea Volcano, Hawaiʻi. Bull. Volcanol. 73, 1179–1186.

Patrick, M.R., Orr, T.R., Antolik, L., Lee, R., Kamibayashi, K., 2012. Recent improvements in monitoring Hawaiian volcanoes with webcams and thermal cameras. In: Fall Meeting of the American Geophysical Union, San Francisco, December 3–7, Abstract V33E-01.

Poland, M.P., Sutton, A.J., Gerlach, T.M., 2009. Magma degassing triggered by static decompression at Kīlauea Volcano, Hawaiʻi. Geophys. Res. Lett. 36, L16306.

Rivalta, E., Segall, P., 2008. Magma compressibility and the missing source for some dike intrusions. Geophys. Res. Lett. 35, L04306.

Sawyer, G.M., Carn, S.A., Tsanev, V.I., Oppenheimer, C., Burton, M., 2008. Investigation into magma degassing at Nyiragongo volcano, Democratic Republic of Congo. Geochem. Geophys. Geosyst. 9, Q02017.

Spampinato, L., Oppenheimer, C., Calvari, S., Cannata, A., Montalto, P., 2008. Lava lake surface characterization by thermal imaging: Erta ʼAle volcano (Ethiopia).

Geochem. Geophys. Geosyst. 9, Q12008.

Swanson, D., Wooten, K., Orr, T., 2009. Buckets of ash track tephra flux from Halemaʻumaʻu Crater, Hawaiʻi. Eos 90, 427.

Talwani, M., 1973. Computer usage in the computation of gravity anomalies. Methods Comput. Phys. 13, 343–389.

Tazieff, H., 1994. Permanent lava lakes: Observed facts and induced mechanisms. J. Volcanol. Geotherm. Res. 63, 3–11.

Tedesco, D., Vaselli, O., Papale, P., Carn, S.A., Voltaggio, M., Sawyer, G.M., Durieux, J., Kasereka, M., Tassi, F., 2007. January 2002 volcano-tectonic eruption of Nyiragongo volcano, Democratic Republic of Congo. J. Geophys. Res. 112, B09202.

Wilson, D., Elias, T., Orr, T., Patrick, M., Sutton, J., Swanson, D., 2008. Small explosion from new vent at Kīlauea's summit. Eos 89 (22), 203.

Witham, F., Llewellin, E.W., 2006. Stability of lava lakes. J. Volcanol. Geotherm. Res. 158, 321–332.

Witham, F., Woods, A.W., Gladstone, C., 2006. An analogue experiment model of depth fluctuations in lava lakes. Bull. Volcanol. 69, 51–56.

Wooten, K.M., Thornber, C.R., Orr, T.R., Ellis, J.F., Trusdell, F.A., 2009. Catalog of tephra samples from Kīlauea's summit eruption, March–December 2008. U.S. Geol. Surv. Open-File Rep. 2009-1134.

XMLVIEW: extended

Appendix A. Supplementary material

The following is the Supplementary material related to this article.

begin ecomponent begin ecomponent begin ecomponent begin ecomponent begin ecomponent begin ecomponent begin ecomponent begin ecomponent begin ecomponent begin ecomponent begin ecomponent begin ecomponent begin ecomponent begin ecomponent begin ecomponent begin ecomponent begin ecomponent begin ecomponent

`Label`: Video 1

`caption`: The movie shows images from the thermal camera that looks into the summit vent (Fig. 1) taken during the March 2011 draining event. Images from the thermal camera have been synchronized with the gravity signal observed at station HOVL-G (Fig. 1). Note that Hawaiian Standard Time is imprinted on the thermal camera images, while times in the gravity sequence are GMT (Hawaiian Standard Time minus 10 hours).

`link`: **VIDEO : mmc1**

end ecomponent end ecomponent end ecomponent end ecomponent end ecomponent end ecomponent end ecomponent end ecomponent end ecomponent end ecomponent end ecomponent end ecomponent end ecomponent end ecomponent end ecomponent end ecomponent end ecomponent end ecomponent

Highlights

- In March 2011, the lava lake of Kīlauea drained as magma fed a lateral intrusion.
- The lava level drop was tracked by geological and geophysical measurements.
- Lava density is calculated from the observed gravity and lava level changes.
- The resulting density (950 ± 300 kg m^{-3}) indicates that the lava lake is gas-rich.
- Knowledge of density is key to understanding lava lake convection and degassing.